

Superconductivity and Electronic Properties of Mg-Cd and Some hcp Mg Alloys

E. Bucher, V. Heine,* K. Andres, J. P. Maita, and A. S. Cooper

Bell Telephone Laboratories, Murray Hill, New Jersey 07974

(Received 20 December 1971)

The superconducting transition temperature T_c , electronic specific heat γ , and Debye temperature Θ have been measured in the Mg-Cd alloy system and in some other Mg-rich hcp alloys. No superconductivity could be detected in the latter above 0.013 °K. On the Cd-rich side of the Cd-Mg system T_c drops rapidly on alloying with Mg, and if one correlates this with the drop in c/a , one may expect Mg to have T_c around 1×10^{-4} °K. A subsidiary maximum in T_c occurs at $x=0.20$ (in $\text{Mg}_x\text{Cd}_{1-x}$), where γ and Θ have a marked maximum and minimum, respectively. At $x=0.50$, the γ has a minimum and Θ has a maximum if the mass factor is divided out. The possible origin of the anomaly at $x=0.20$ is discussed in terms of ordering and an incipient instability reflected in the rapid variation of c/a .

I. INTRODUCTION

The present work is an experimental investigation of some electronic properties of hcp metals and alloys in relation to their crystal structure, in particular the c/a ratio and the presence of ordering in alloys. The original motivation was the lack of any observation of superconductivity in Mg down to 0.004 °K although a higher T_c might be expected from comparison with Be, Zn, and Cd.

The question of the possible relationship between anomalous c/a ratios in hcp alloys and their electronic properties was first discussed by Hume-Rothery and Raynor.¹ However, since all the elements Be, Mg, Zn, Cd and the Cd-Mg alloys have the same electron per atom ratio $z = 2$, it was not possible for the discussion to be very explicit until more detailed information became available about the differences in atomic potentials between these elements. Weaire² indeed found in theoretical calculations that in Zn and Cd the total energy of the system (ions and conduction electrons) becomes a minimum at the c/a values considerably greater than the ideal ratio $(c/a)_0 = (\frac{8}{3})^{1/2} = 1.63$. His calculations, based on the Heine-Abarenkov model potential reproduced quite well the rapid drop in c/a as Cd is alloyed with Mg until it remains nearly constant around the ideal value for a Mg concentration x (in $\text{Mg}_x\text{Cd}_{1-x}$) greater than about 0.3 or 0.4. (See Fig. 2 below for a reproduction of the data.) He also predicted³ a minimum of the elastic constant

$$C' = C_{11} + C_{12} + 2C_{33} - 4C_{13} \quad (1)$$

in disordered $\text{Mg}_x\text{Cd}_{1-x}$ alloys around $x=0.3-0.4$.

There are, of course, many other interesting relations between band-structural and electronic properties such as electronic specific heat γ , superconducting transition temperature T_c , electron-electron and electron-phonon interactions, etc. It has been a puzzle for a long time that Mg

does not exhibit superconductivity down to 0.004 °K⁴ although calculations^{5,6} that are quite successful for Zn and Cd would indicate $T_c = 0.012$ °K for Mg.^{5,6} For Li the prediction of superconductivity failed likewise.^{4,7} It must be emphasized of course that difficulties in predicting new low-temperature superconductors grow exponentially with decreasing T_c because of the critical balance between the attractive electron-phonon parameter λ and the repulsive screened-Coulomb term μ^* , and the exponential dependence of T_c on them.

Although a direct search for superconductivity in Mg (and Li) in the course of this work led to negative results down to 0.004 °K,⁴ we feel it worthwhile to present here the same problem from a different point of view by measuring some related electronic properties of a relevant alloy system. We choose for Mg the simplest and most conclusive one, the Cd-Mg system, which exhibits complete miscibility at high temperatures in the hcp phase.⁸ At room temperature there are three ordered phases with extended homogeneity ranges, Cd_3Mg , CdMg , and CdMg_3 , all closely related to the hcp structure.⁸

The method of investigation follows earlier work.⁹ T_c is followed to the highest Mg concentration while the electronic specific heat γ and the Debye temperature Θ were also measured. Unfortunately, superconducting-tunneling data are not available since it is not a strong-coupling system. Various derived parameters are then plotted against Mg concentration x in the hope that these will allow a reasonable extrapolation to pure Mg in order to predict its T_c .

As it turned out, extrapolation is rendered difficult by anomalies in all the parameters around $x=0.20$. For example, T_c has a subsidiary maximum. This occurs at the transition from the disordered Cd-rich hcp phase to the ordered Cd_3Mg phase. But it also coincides with the most rapid variation of c/a with concentration x . Let us ex-

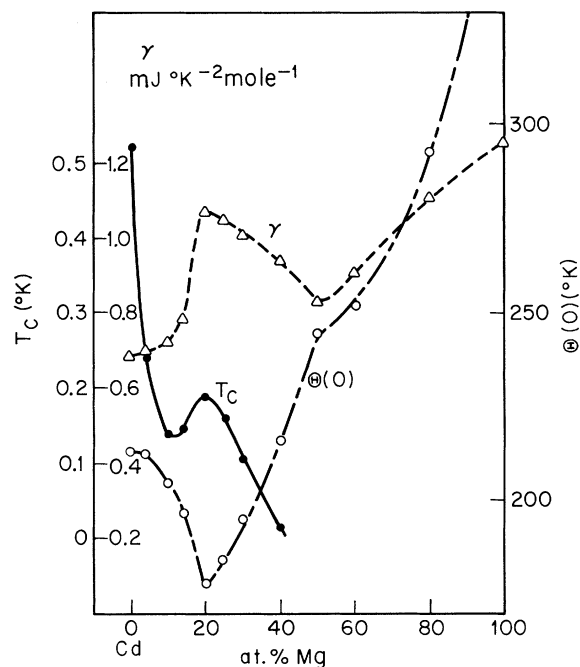


FIG. 1. Measured quantities: superconducting transition temperature T_c , electronic specific heat γ , and Debye temperature Θ at 0 °K.

pand the total energy U in terms of the deviation

$$\eta = (c/a) - (c/a)_0$$

of c/a from the ideal value:

$$U = A + B\eta + C\eta^2 + \dots \quad (2)$$

The linear term is small and will be neglected.² Then Weaire² showed that at the Mg-rich end of the phase diagram, C is positive resulting in c/a near ideal. But C becomes negative for Mg concentrations x less than about 0.3, so that the ideal hcp structure is unstable and distorts to a considerably larger c/a . These may therefore be analogies here with other superconductors where the maximum T_c and lattice instability also seem to go hand in hand.¹⁰⁻¹⁴

II. EXPERIMENTAL RESULTS

All Mg alloys were prepared in degassed and sealed tantalum crucibles ($\frac{1}{2}$ -in. o.d.) by resistance heating. After alloying, the tantalum was peeled off and the ingot turned to a cylindrical button of $\frac{7}{16}$ in. diam and $\frac{1}{4}$ in. long for specific-heat measurements in a heat-pulse calorimeter described previously.¹⁵ On the same specimen superconductivity was detected by a low-frequency (28 Hz) mutual-induction technique in a field of 0.2 Oe. We found it impossible to keep the Mg-Cd alloys disordered at low temperature, even by quenching from slightly below the solidus curve to

liquid nitrogen. Therefore, the samples were cooled slowly down to room temperature and kept there for several days and then cooled further over a period of 18 h down to 20 °K, in order to allow the samples to reach thermodynamic equilibrium. Unfortunately, the degree of chemical order at low temperatures is unknown to us and might be guessed from the low-temperature properties themselves, except for Cd_3Mg which was nearly perfectly ordered even at 296 °K. However, this is unimportant (see Sec. III and Ref. 19). The results of the Cd-Mg system are shown plotted in Fig. 1 and summarized in Table I. The specific-heat (C_p) measurements were carried out from 1.5 to 40 °K and the low- T Debye temperature $\Theta(T)$ defined by the usual relation

$$C_p/T = \gamma + \frac{12}{5} \pi^4 R T^2 / \Theta^3(T) \quad (3)$$

The values $\Theta(0)$ extrapolated to absolute zero are included in Table I, while Table II shows the temperature dependence of $\Theta(T)$ for representative samples. The γ values for pure Mg and pure Cd agree well with earlier determinations.¹⁶⁻¹⁸

III. ANALYSIS OF RESULTS

The observed superconducting T_c and electronic specific heat γ are both compounded of various physical effects, which are necessary to unravel as far as possible in order to draw meaningful conclusions from the data.

We start by following the BCS theory of superconductivity to write

$$T_c = 1.14 \Theta e^{-1/\epsilon_{\text{BCS}}} \quad (4)$$

$$g_{\text{BCS}} = \eta V \quad (5)$$

where $\eta = \eta(E_F)$ is the density of states at the Fermi level and V the net, attractive, electron-phonon interaction. If we further follow BCS and ignore the electron-phonon enhancement of γ , then γ is proportional to η and $V' = g_{\text{BCS}}/\gamma$, a measure of V . Figure 2 shows g_{BCS} and g_{BCS}/γ vs composition x . The latter has a somewhat smoother variation with x and a more definite trend than T_c (Fig. 1), γ (Fig. 1), or g_{BCS} (Fig. 2), and its rapid drop with x from the high value in pure Cd suggests a correlation with c/a also shown in Fig. 2, taken from Ref. 1.

It must be emphasized of course that all samples containing more than 10-at.% Mg are ordered phases. It appears that g_{BCS}/γ is not particularly sensitive to chemical order, confirming general observations¹⁹ that the BCS parameter V is usually quite insensitive to structural parameters. The structural dependence of T_c derives mostly from that of η . We therefore feel encouraged not to worry too much about chemical order and we treat the whole CdMg system as if it were an ideal solid-solution system (as is true at higher temperatures).

TABLE I. The measured superconducting transition temperature T_c , Debye temperature Θ , and electronic specific heat γ , with derived quantities.

Alloy	T_c (°K)	$\Theta(0)$ (°K)	γ mJ/°K ² mole	g_{BCS} [Eq. (4)]	λ [Eqs. (6) and (7)]	Structure
Cd	0.52	213	0.69	0.165	0.386	hcp
Cd _{0.96} Mg _{0.04}	0.24	212	0.705	0.145	0.348	
Cd _{0.90} Mg _{0.10}	0.138	205	0.725	0.134	0.334	
Cd _{0.86} Mg _{0.14}	0.145	197	0.795	0.136	0.340	hex ordered
Cd _{0.80} Mg _{0.20}	0.185	178	1.07	0.145	0.360	Cd ₃ Mg
Cd _{0.75} Mg _{0.25}	0.160	185	1.05	0.139	0.357	$2c/a=1.62$
Cd _{0.70} Mg _{0.30}	0.105	195	1.01	0.130	0.343	
Cd _{0.60} Mg _{0.40}	0.016	216	0.942	0.103	0.299	orthorhombic
Cd _{0.50} Mg _{0.50}	<0.015	245	0.835	<0.101	...	CdMg
Cd _{0.40} Mg _{0.60}	<0.015	252	0.904	<0.101	...	
Cd _{0.20} Mg _{0.80}	<0.015 ⁽⁴⁾	293	1.10	<0.099	...	hex CdMg ₃
Mg	<0.004	382	1.25	<0.087	...	hcp
Mg _{0.82} In _{0.18}	<0.013	273	1.23	<0.096		hcp
Mg _{0.89} Al _{0.11}	<0.013					
Mg _{0.97} Ga _{0.03}	<0.013					
Mg _{0.85} Tl _{0.15}	<0.013					
Mg _{0.93} Pb _{0.07}	<0.013					
Mg _{0.97} Zn _{0.03}	<0.013					
Mg _{0.97} Sn _{0.03}	<0.013					

In order to undertake a more detailed discussion and relate to theoretical calculations of T_c , we also analyze the data according to McMillan's

formulas²⁰:

$$T_c = 0.69 \Theta e^{-1/g_{MM}} \quad (6)$$

$$g_{MM} = \frac{\lambda - \mu^*(1 + \alpha\lambda)}{\beta(1 + \lambda)} \quad (7)$$

where

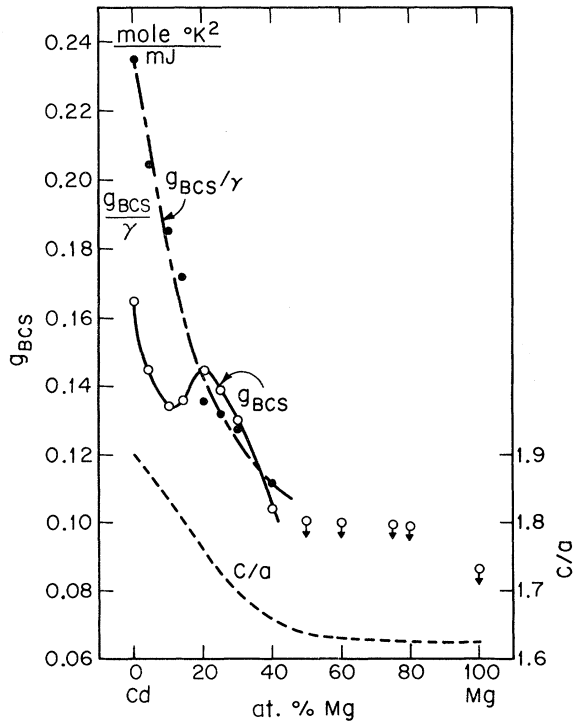
$$\alpha = 0.62, \quad \beta = 1.04 \quad ,$$

although they were derived for strong-coupling superconductors such as Nb with a bcc frequency spectrum. Here λ is the electron-phonon interaction parameter which also enters the phonon enhancement of the electronic specific heat:

$$\gamma = \frac{2}{3} (\pi k)^2 \eta(E_F)(1 + \lambda) \quad (8)$$

TABLE II. Variation of Debye Θ with temperature. The composition of the alloys is indicated in at. % Mg.

T (°K)	Pure Cd	10%	20%	50%	Pure Mg
0	213	206	178	244	382
2	195	204	178	244	382
4	168	185	177	236	382
6	140	159	174	226	381
8	128	149	167	214	380
10	125	142	163	202	378.5
12	125	141	159	195	371.5
14	126	143	158	191	364
16	128	145	159	189	361
18	131	146.5	161	188	355
20	133	148	164	188	349

FIG. 2. g_{BCS} and the correlation of g_{BCS}/γ with c/a from Ref. 1.

η is the bare density of states including band effective masses. λ in turn is related²⁰ to the electron-phonon coupling V_p by $\lambda = \eta V_p$, so that dropping constant factors we may take

$$V_p = \lambda(1 + \lambda)/\gamma \quad (9)$$

as a measure of the interaction strength, analogous to V in the BCS theory. The screened-Coulomb repulsion μ^* is given by²¹

$$\mu^* = \frac{\mu}{1 + \mu \ln E_F/k\Theta} \quad (10)$$

$$\lambda = \frac{\beta g}{2} \frac{2(1 - \beta g) + \xi \beta g(1 + \alpha) + \xi^{1/2} \{4[1 - \beta g(1 - \alpha)] + \xi(\beta g)^2(1 - \alpha)^2\}^{1/2}}{(1 - \beta g)^2 - \alpha \xi(\beta g)^2} \quad (11)$$

and

$$\mu^* = \beta g \left(\xi \frac{1 + \lambda}{1 + \alpha \lambda} \right)^{1/2} \quad (12)$$

For Cd, ξ was found to be 0.36 by Palmy²² and 0.23 by Fassnacht and Dillinger.²³ This leads to $\lambda = 0.406$ and $\mu^* = 0.117$ or $\lambda = 0.366$ and $\mu^* = 0.0933$, respectively, and we take the mean values $\mu^* = 0.106$ and $\lambda = 0.386$. A theoretical calculation⁷ gave $\mu^* = 0.11$ for Cd, in good agreement with experiment, and 0.16 for Mg. We therefore took for the alloys a linear interpolation between the latter value for Mg and the experimental value for Cd. The other parameters λ can now be calculated from (6) and (7) and η from (8). To test whether the assumption of linear interpolation created serious errors, we tried other intermediate forms and found that they did not alter materially the shape of the curve of V_p against x . We show in Fig. 3 the three quantities V_p , λ , and η .

IV. DISCUSSION OF ELASTIC DATA

The measured Debye temperature Θ ($T=0$) for the Cd-Mg alloys is displayed graphically in Fig. 4 as a function of Mg concentration x . These are Θ values derived from (3) and extrapolated to absolute zero. The reduced Debye temperature

$$\Theta_r = \Theta(\bar{M}/M_{Cd})^{1/2}, \quad (13)$$

where \bar{M} is the mean atomic mass in the alloy, is more directly a measure of the elastic forces: The low- T values of Θ_r are also plotted in Fig. 4.

Comparison with Fig. 1 shows immediately that Θ_r has a minimum at $x = 0.2$ and maximum at $x = 0.5$, where γ has a maximum and minimum, respectively, a correlation also found in other alloy systems.²⁴ From Fig. 3 we note that the peak in γ still remains a peak in $\eta(E_F)$ when the phonon enhancement factor is divided out, and we assume the same is true for the minimum at $x = 0.5$ though the superconductivity data do not extend as far as

in terms of μ the unscreened interaction.

Since we have three items of experimental information Θ , T_c , and γ , and a theory with four parameters Θ , η , λ , and μ^* , it is necessary to make some assumptions about μ^* , the least significant of these. For pure Cd the λ and μ^* can be calculated from the measured isotope shift^{22, 23} where we have

$$T_c \propto M^{-(1-\epsilon)/2}$$

in the usual notation. Both λ and μ^* can be expressed in terms of $g_{MM}(=g)$ and ξ :

that. (This of course in itself is evidence of a small λ and hence small correction factor $1 + \lambda$.)

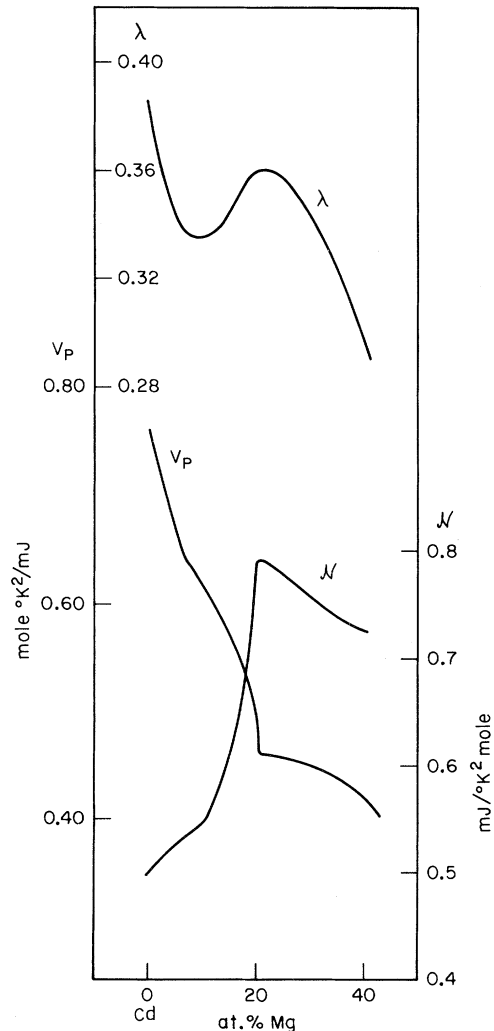


FIG. 3. Parameters λ , η , and V_p from the McMillan theory.

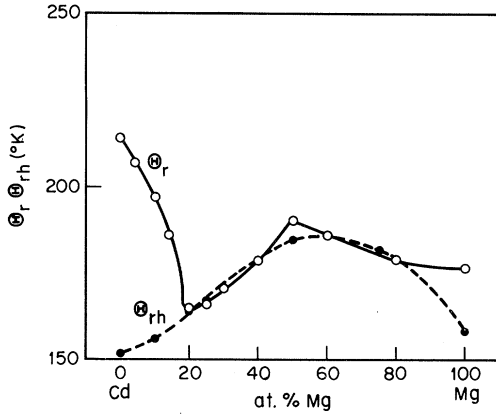


FIG. 4. Reduced Debye temperature Θ_r at 0°K, and the corresponding Θ_{rh} from (19) for the high- q phonons.

In the following discussion we therefore take γ to be simply a measure of $\eta(E_F)$.

The correlation between Θ and γ (or η) is easily explained following ideas of Fuchs.²⁵ It has been known for a long time that the Fermi energy of the electron gas makes a contribution C_e to the elastic bulk modulus of a metal, given by

$$C_e = V \frac{d^2 U_e}{dV^2} = \frac{n^2}{\eta(E_F)}, \quad (14)$$

where n is the density of electrons. Thus a high density of states means the electron gas is more compressible, yielding a low Θ . We have not found a good discussion of (14) in the literature and may perhaps be excused in the following simple derivation. Let u be the electronic energy *per unit volume* of metal. If we add electron *density* dn , we have $du = E_F dn$ by definition of E_F , i. e.,

$$\frac{du}{dn} = E_F. \quad (15)$$

Differentiating again we have

$$\frac{d^2 u}{dn^2} = \frac{dE_F}{dn} = \frac{1}{\eta(E_F)} \quad (16)$$

by definition of $\eta(E_F)$, which is taken again per unit volume. On compressing a material, the change in $n = N/V$ comes through change in V for a fixed total number N of electrons:

$$\frac{dn}{dV} = -\frac{N}{V^2} = -\frac{n}{V}. \quad (17)$$

The result (14) now follows by mechanically differentiating the total energy $U_e = Vu(n)$ of a given mass of material:

$$\begin{aligned} \frac{dU_e}{dV} &= u + V \frac{du}{dn} \frac{dn}{dV} \\ &= u - nE_F, \end{aligned} \quad (18)$$

$$V \frac{d^2 U_e}{dV^2} = V \left(\frac{du}{dn} - E_F - n \frac{dE_F}{dn} \right) \frac{dn}{dV}.$$

In the last equation the first two terms cancel by (15) and the last term reduces to the desired result with the aid of (16) and (17). In this argument the band structure and $\eta(E)$ are assumed to remain unchanged under compression, as in a noninteracting free-electron gas. That is of course unrealistic but nevertheless (14) remains as an identifiable contribution from the Fermi energy of filling electron states, among many other terms in the total elastic constant. The anticorrelation between Θ and γ cannot therefore be made more quantitative.

There is an alternative possible mechanism for the minimum in Θ . We have seen that the elastic constant $C'(1)$ is expected to have a deep minimum³ (though not to go completely to zero). Weaire's calculations are not accurate enough to locate reliably the concentration at the minimum, but it must coincide with the point where c/a increases rapidly with decreasing x . In disordered alloys at room temperature this starts at $x = 0.3-0.4$, but the maximum slope is at $x = 0.2$ (Fig. 2). Indeed at low temperature, c/a remains near ideal down to $x = 0.14$ (Table I). It is therefore reasonable to expect the minimum in C' and hence in Θ around $x = 0.2$.

These two arguments are quite separate, (14) referring to the bulk modulus and C' being a shear modulus. Which explanation is correct? Both are. Recent measurements²⁶ of the elastic constants of Cd-rich Cd-Mg alloys show that they all decrease rapidly with x , including the bulk modulus and the particular shear constant $C'(1)$. If we ignore the anomaly in the data²⁶ at $x = 0$, which we believe to be spurious, then the C_{ij} drop by factors from 0.45 to 0.86 between $x = 0.005$ and $x = 0.14$ at room temperature, whereas Θ_r^2 drops by a factor of 0.77 at low temperature, which we regard as satisfactory agreement.

We turn now to the temperature dependence of $\Theta(T)$. For pure Mg there are considerable differences between various published values,¹⁷ ranging for $\Theta(0)$ from 342 to 440°K, our value of $\Theta(0) = 382$ °K agreeing best with the measurement of Slutsky and Garland.²⁷ Above 15°K our $\Theta(T)$ agrees perfectly with earlier values.²⁸

The temperature dependence from Table II is plotted in reduced form $\Theta(T)/\Theta(0)$ in Fig. 5. $\Theta(0)$ characterizes the phonons of small wave number q with frequencies $\omega(q)$ determined by the elastic constants, whereas $\Theta(T)$ at higher T characterizes the phonon distribution as a whole dominated by the large- q phonons. The temperature variation in Fig. 5 is unusually strong for low Mg concentrations and around 50-at.% Mg, $\Theta(T)$ drops well be-

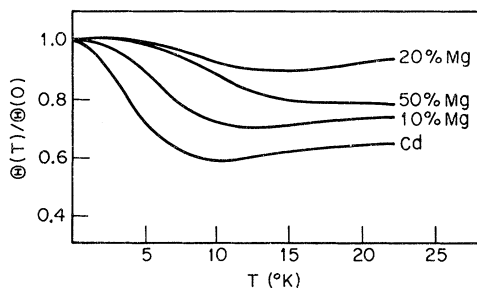


FIG. 5. Temperature dependence of the Debye temperature.

low $\Theta(0)$ before beginning its usual linear rise. We conclude that for these concentrations the elastic constants are unusually stiff compared with the phonon distribution as a whole. This is consistent with our remarks about the relation between $\Theta(0)$ and γ [see Eq. (14)]. In this connection we note that the free-electron value of γ for pure Cd is $0.95 \text{ mJ } ^\circ\text{K}^{-2} \text{ mole}^{-1}$ without electron-phonon enhancement. Taking into account the enhancement factor $1 + \lambda$ in (8), we see that the correct description of Fig. 1 is that γ for Cd and $\text{Cd}_{0.50}\text{Mg}_{0.50}$ is low, rather than that for $\text{Cd}_{0.80}\text{Mg}_{0.20}$ being high. The compressibility at these concentrations from (14) is therefore low, making the low- q phonons hard, in agreement with our conclusion from Figs. 4 and 5.

We can take the analysis one step further and try to derive a Θ including the higher- q phonons. One can define a reduced Debye temperature Θ_{rh} at higher temperatures (including higher- q phonons) in the following arbitrary way: We determine experimentally the temperature $T_{1/2}$ for which the lattice specific heat reaches $\frac{1}{2}$ of the equipartition value $3R$. In our case the correction for the electronic specific heat is negligible. On the other hand, we know from the Debye function that for $\Theta/T = 4.02$ we have $C_L = \frac{3}{2}R$. Therefore, we define

$$\Theta_{\text{rh}} = 4.02 T_{1/2} (\bar{M}/M_{\text{Cd}})^{1/2}, \quad (19)$$

reducing all Θ values at the same time with respect to the Cd mass. \bar{M} is the average atomic mass of the alloy. For pure Mg and CdMg_3 , we used the data of Ref. 28 which on the Cd side are in good agreement with our results. Θ_{rh} and Θ_r , the reduced low- q Debye temperature, are plotted in Fig. 4. Besides the strong difference in lattice softness for low and high q 's, we notice a slight drop in Θ_{rh} at the Cd side. This is qualitatively consistent with a stronger electron-phonon interaction as seen in T_c on the Cd-rich side because the electron-phonon interaction describes the screening of the ions and hence lowers the phonon frequencies. The trend is also consistent with the behavior of c/a because the pseudopotential gives a negative con-

tribution to C in (2), being sufficiently large at the Cd end of the phase diagram to drive C negative and hence produce the deviation of c/a from the ideal value as described in Sec. I.

V. DISCUSSION OF SUPERCONDUCTIVITY RESULTS

We consider first the absence of superconductivity in Mg down to $0.004 \text{ }^\circ\text{K}$, although from its electronic specific heat γ and Debye temperature Θ we might expect it to be more favorable for superconductivity than other hexagonal superconductors such as Be, Zn, and Cd. For instance both γ and Θ are larger for Mg than Cd (Fig. 1).

The hcp Mg-rich alloys Mg- X ($X = \text{Zn, Al, Ga, In, Tl, Sn, Pb}$) turned out to be not very much help in analyzing this question, not showing any superconductivity down to $0.013 \text{ }^\circ\text{K}$. Their concentrations all correspond to the maximum solid solubility. Only alloys with simple metals were considered because in Mg-Sc, for instance, the possible complication of d electrons would lead to inconclusive results about pure Mg. The alloy (18-at. % In) with highest electron concentration $\lambda = 2.18$ is perhaps the most instructive. Its γ is slightly lower than that of pure Mg, probably going through a shallow minimum with composition as does¹⁶ Mg-Al. The fact that there is so little change even for a reasonable change in electron concentration shows there is nothing special about pure Mg itself as regards γ , and the same is presumably implied for the separate factors $\eta(E_F)$ and $1 + \lambda$.

We therefore explored the full Cd-Mg phase diagram to try to reach more definite conclusions. As can be seen in Figs. 1 and 2, neither T_c nor g_{BCS} are suitable parameters for a possible extrapolation to pure Mg. The fact, of course, that superconductivity of Cd disappears relatively quickly upon alloying with Mg makes precise predictions almost impossible. The only hope would seem to lie in correlating the unrenormalized BCS parameter with c/a of the alloy system, which shows rather similar behavior (Fig 2). For this purpose we use the high-temperature disordered c/a data because they are more likely to correspond to the chemical composition, whereas the lower values for some alloys at low temperature (Table I) may be due to ordering effects. If we write, tentatively,

$$r(x) = r_{\text{Mg}} + \Delta r(x) \quad (20)$$

and

$$V'(x) = V'_{\text{Mg}} + \alpha \Delta r(x), \quad (21)$$

where $r = c/a$, $x = \text{alloy composition}$, and $V' = g_{\text{BCS}}/\gamma$ and calculate α from the initial linear slope between Cd and $\text{Cd}_{0.75}\text{Mg}_{0.25}$ taken from Fig. 2, we find for Mg that $g_{\text{BCS}} = 6.7 \times 10^{-2}$ and $T_c \approx 10^{-4} \text{ }^\circ\text{K}$.

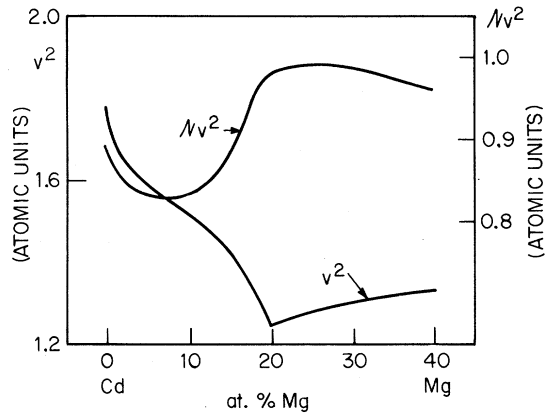


FIG. 6. Parameters v^2 and ηv^2 (in arbitrary units) from the McMillan theory.

Theoretical g_{BCS}/γ values for $x > 0.25$ calculated on the basis of expressions (19) and (20) however yield much too low values in the region up to 40-at. % Mg where a comparison with experimental numbers can be made. One may excuse this discrepancy of course by some structural dependence of V , which is much more pronounced in McMillan's theory (Fig. 3) and that the lower V 's could correspond to the disordered hcp phase. At the moment one cannot draw more conclusion from our data unless one produces hcp disordered Cd-Mg alloys (possibly by evaporation on a cold substrate) and measures their T_c 's to verify (19) and (20). But this is probably as elaborate as trying to measure T_c of pure Mg itself. With recently improved nuclear-cooling techniques²⁹ it should be possible to extend measurements down to 10^{-4} °K or even lower. Probably the relation between g_{BCS}/γ and c/a is much more complicated than assumed by (20) and (21). From basic ideas on superconductivity g_{BCS}/γ is a measure of the electron-phonon coupling as expressed in terms of the pseudopotential and the deviation of c/a from ideal is also the result of a strong pseudopotential as discussed in Sec. IV. We therefore expect some connection between them, but each depends on the pseudopotential in too complicated a way for us to say how direct the relationship should be. It may be worthwhile to mention here a similar relationship between anomalous c/a ratios and T_c in hcp noble-metal alloys.^{30,31} In contrast to the Cd-Mg system these alloys exhibit c/a ratios below the ideal value $(\frac{8}{3})^{1/2}$.³¹ T_c increases monotonously with increasing deviations from $(\frac{8}{3})^{1/2}$. The origin of this empirical relation may again be found in pseudopotential considerations which in turn might also explain

why hcp Be with its anomalously low c/a ratio again becomes superconducting at 26 m °K although its γ, θ parameters together are less favorable than for Mg, which remains normal down to 4 m °K.

We turn now to the subsidiary maximum in T_c at a concentration $x = 0.20$. Maxima in T_c are often associated with instabilities, and it would be nice if the relative simplicity of the MgCd system and the measurement of three quantities T_c , γ , and Θ would enable us to unravel what factors are most responsible. We first consider λ , V_p , and η in Fig. 3. They all show anomalies. As we have already remarked, η is very low for Cd, dropping rapidly for $x < 0.2$, and this is correlated with the jump in c/a near ideal to about 1.9. (Note that in our annealed alloys at low temperatures there is a discontinuity or rapid variation of c/a between $x = 0.1$ and 0.2, unlike the more spread out change shown in Fig. 2 for disordered alloys at high temperature.) The drop in η is presumably due to the fact that the $[1\bar{1}01]$ type of reciprocal-lattice vectors become nearly equal to the diameter of the Fermi sphere,^{32,33} produce band gaps near the Fermi level, and hence eliminate a substantial fraction of the Fermi surface. To carry the analysis one step further, we note from McMillan's theory that λ should have the form²⁰

$$\lambda = (\text{const})\eta v^2 / \Theta_{\text{rh}}^2, \quad (22)$$

where v is a mean pseudopotential matrix element for scattering on the Fermi surface. Figure 6 therefore shows $v^2 = \lambda \Theta_{\text{rh}}^2 / \eta$ (in arbitrary a. u.). As expected, it is largest for pure Cd, but it still shows an anomaly at $x = 0.2$, presumably because large areas of Fermi surface are eliminated for $x < 0.2$ so that one has a different average. Interestingly enough, the quantity $\eta v^2 = \lambda \Theta_{\text{rh}}^2$ (in arbitrary atomic units) also shown in Fig. 6, has the least over-all variation from pure Cd to $x = 0.4$. This is in accordance with McMillan's unexplained observation in quite different superconducting systems²⁰ that the quantity ηv^2 is more nearly constant than anything else. However, it still shows an anomaly at $x = 0.2$, and we must conclude that the anomaly has no simple explanation. As well as the change in c/a , we have a change from an ordered ($x > 0.2$) to a disordered ($x < 0.1$) structure. Both affect η , v^2 , and the phonon spectrum in a complex way, which then combine to give the subsidiary maximum in T_c (Fig. 1).

ACKNOWLEDGMENT

We would like to thank M. Peter for many interesting comments on this work.

*Permanent address: Cavendish Laboratory, Cambridge, England.

¹W. Hume-Rothery and G. V. Raynor, Proc. Roy.

Soc. (London) A174, 471 (1940).

²D. Weaire, J. Phys. C 1, 210 (1968).

³D. Weaire, Phil. Mag. 20, 1083 (1969).

- ⁴T. L. Thorp, B. B. Triplett, W. D. Brewer, N. E. Phillips, D. A. Shirley, J. E. Templeton, R. W. Stark, and P. H. Schmidt, *J. Low Temp Phys.* **3**, 589 (1970).
- ⁵P. B. Allen and M. L. Cohen, *Solid State Commun.* **7**, 677 (1969).
- ⁶P. B. Allen and M. L. Cohen, *Phys. Rev.* **187**, 525 (1969).
- ⁷T. Schneider, E. Stoll, and W. Buhner, *Helv. Phys. Acta* **42**, 46 (1969). See also Ref. 6, p. 531 for further references.
- ⁸M. Hansen, *Constitution of Binary Alloys* (McGraw-Hill, New York, 1958), p. 425; and R. P. Elliott, *ibid.* Suppl. (McGraw-Hill, New York, 1965), p. 285.
- ⁹K. Andres, E. Bucher, J. P. Maita, and R. C. Sherwood, *Phys. Rev.* **178**, 702 (1969).
- ¹⁰A. D. B. Woods and S. H. Chen, *Solid State Commun.* **2**, 233 (1964).
- ¹¹H. G. Smith and W. Gläser, *Phys. Rev. Letters* **25**, 1611 (1970).
- ¹²R. C. Dynes, *Phys. Rev. B* **2**, 644 (1970).
- ¹³J. C. Phillips, *Phys. Rev. Letters* **26**, 543 (1971).
- ¹⁴C. W. Chu, E. Bucher, A. S. Cooper, and J. P. Maita, *Phys. Rev. B* **4**, 320 (1971).
- ¹⁵F. J. Morin and J. P. Maita, *Phys. Rev.* **129**, 1115 (1963).
- ¹⁶J. A. Rayne, *J. Phys. Chem. Solids* **7**, 268 (1958).
- ¹⁷D. L. Martin, *Proc. Phys. Soc. (London)* **78**, 1482 (1961) and references therein for Mg.
- ¹⁸N. E. Phillips, *Phys. Rev.* **134**, A385 (1964) and references therein for Cd.
- ¹⁹E. Bucher, F. Heiniger, and J. Muller, *Physik Kondensierten Materie* **2**, 210 (1964). An excellent example are the recently studied Cr₃Si phases, see, e.g., P. Spitzli, R. Flukiger, F. Heiniger, A. Junod, J. Muller, and J. L. Staudenmann, *J. Phys. Chem. Solids* **31**, 1531 (1970).
- ²⁰W. L. McMillan, *Phys. Rev.* **167**, 331 (1968).
- ²¹P. Morel and P. W. Anderson, *Phys. Rev.* **125**, 1263 (1962).
- ²²C. Palmy, *Phys. Letters* **29A**, 373 (1969).
- ²³R. E. Fasnacht and J. R. Dillinger, *Phys. Rev. B* **2**, 4442 (1970).
- ²⁴F. Heiniger, E. Bucher, and J. Muller, *Physik Kondensierten Materie* **5**, 243, 1966.
- ²⁵For a discussion of this point see, e.g., J. de Launay, in *Solid State Physics*, Vol. 2, edited by F. Seitz and D. Turnbull (Academic, New York, 1956), p. 273.
- ²⁶P. Maennel and F. Guenther, *Phys. Status Solidi* **3a**, 137 (1970).
- ²⁷L. J. Slutsky and C. W. Garland, *Phys. Rev.* **107**, 972 (1957).
- ²⁸R. S. Craig, C. A. Krier, L. W. Coffey, E. A. Bates, and W. E. Wallace, *J. Am. Chem. Soc.* **76**, 238 (1954).
- ²⁹K. Andres and E. Bucher, *J. Appl. Phys.* **42**, 1522 (1971).
- ³⁰H. L. Luo and K. Andres, *Phys. Rev. B* **1**, 3002 (1970).
- ³¹T. B. Massalski, *J. Phys. Radium* **23**, 647 (1962).
- ³²V. Heine and D. Weaire, *Phys. Rev.* **152**, 603 (1966).
- ³³V. Heine and D. Weaire, in *Solid State Physics*, Vol. 24, edited by F. Seitz and D. Turnbull (Academic, New York, 1970), p. 249.

Dynamic Structure of Vortices in Superconductors. II. $H \ll H_{c2}$ †

Chia-Ren Hu and Richard S. Thompson

Department of Physics, University of Southern California, Los Angeles, California 90007

(Received 22 February 1972)

The time-dependent Ginzburg-Landau equations applicable to a gapless superconductor containing a high concentration of paramagnetic impurities are solved to find the field and charge distributions around an isolated vortex moving in a transport current. The initial slope of the flux-flow resistance with respect to the average magnetic field is found to be approximately $\frac{1}{3}$ the normal resistance divided by H_{c2} . A backflow current is generated for all physical values of the parameters, vanishing only for a special case not possible for this system.

I. INTRODUCTION

In a previous paper¹ we solved a complete set of time-dependent Ginzburg-Landau (GL) equations to find the local current, charge, and field distributions when a transport current is forced through a superconductor in the mixed state near the upper critical magnetic field H_{c2} . This explicit solution was obtained by linearizing the equations in the order parameter, which becomes small as H_{c2} is approached. In the present paper we extend our work to lower magnetic fields, particularly to

quite low fields where the vortices are well separated and may be studied individually. Our method of approaching this problem must be different from before owing to the nonlinearity of the GL equations, since explicit analytic solutions for the spatial dependence of the order parameter and magnetic field have not been obtained even in the static case when no transport current is applied. The equations can be linearized in the regions near and far from the vortex core, and explicit features of the solution are obtained. However, not enough information is obtained from these asymptotic solutions to deter-